CARBURIZATION, CARBIDE FORMATION, METAL DUSTING, COKING

NAOGLJIČENJE, TVORBA KARBIDOV, KOVINSKO UPRAŠENJE, KOKSANJE

Hans Jürgen Grabke

Max-Planck-Institut für Eisenforschung GmbH, Max-Planck-Str. 1, D-40237 Düsseldorf, Germany
grabke@mpie.de

The kinetics of carbon transfer in the carburization of iron and steels is described, considering the surface reactions, their rate equations and their retardation by surface active, adsorbed or segregated elements. Furthermore, the mechanisms and morphologies of corrosion processes are presented which can be caused by carbon; the internal carbide formation in high alloy steels at $a_C < 1$ and "metal dusting", a disintegration of metals and alloys to a dust of graphite and metal particles due to carburization at $a_C > 1$. Fine metal particles cause carbon deposition, thus metal dusting induces the annoying phenomenon "coking".

Keywords: carburization, carbon transfer, steels, surface reactions, high temperature corrosion, internal carbide formation, metal dusting, sulfur effect.

Opisana je kinetika prenosa ogljika pri naogljičenju železa in jekel, ob upoštevanju reakcij na površini, njihove enačbe kot tudi zakasnitev, ki jo povzročajo površinsko aktivni adsorbirani oziroma segregirani elementi. V nadaljevanju je prikazan mehanizem in morfologija korozijskih procesov, ki jih lahko povzroči ogljik, notranja tvorba karbidov pri visokolegiranih jeklih pri $a_C < 1$ in "kovinsko uprašenje", degradacija kovin in zlitin v prah in grafit ter kovinske delce zaradi naogljičenja pri $a_C > 1$. Drobni kovinski delci povzročajo nanos ogljika, tako kovinsko prašenje inducira neželen pojav "koksanja".

Ključne besede: naogljičenje, prenos ogljika, jekla, reakcije na površini, visokotemperaturna korozija, tvorba karbidov, kovinsko uprašenje, učinek žvepla

1 INTRODUCTION

The system Fe-C is of high technical importance and also of great scientific interest, not only because of the existence of the stable system Fe-graphite and the unstable system Fe-cementite, and in addition all the various microstructures which can be attained by different C-contents and heat treatments. Also the reactions and processes in the carburization of iron and steels in gases are very complex and most interesting as will be demonstrated in this paper. Furthermore there are different corrosion processes caused by carburization, i.e. internal carbide formation in high alloy steels in carbonaceous environments and 'metal dusting', a disintegration of metallic materials into a dust of graphite and metal particles in strongly carburizing atmospheres.

In carburizing atmospheres carbon is transferred into solid solution in α- or γ-iron, this process is named carburization and leads at $a_C < 1$ ($a_C = 1$, in equilibrium with graphite) to very well-known equilibria [1]. But also a technical process is called 'gas carburization', in this process low alloy steels are heat treated in carburizing atmospheres for carbon transfer into a surface layer, followed by controlled quenching, i.e. the 'case hardening' of tooth wheels, shafts etc. The kinetics of this carburization is controlled by combined surface reaction and diffusion in the work piece [1,2].
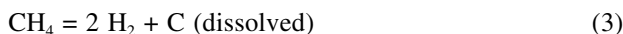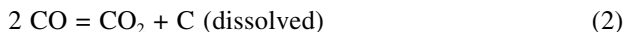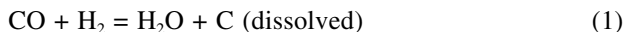
The corrosion process 'carburization' occurs by ingress of carbon into high alloy steels and subsequent internal carbide formation, which embrittles the steels and causes crack formation and loss of oxidation resistance [3,4]. In the high alloy steels, e.g. Alloy 800 (rolled 20Cr-32Ni-steel) or HK40 (cast 25Cr-20Ni-steel) the chromium is precipitated in the carbides $M_{23}C_6$ and M_7C_3 (M = Cr, Fe, Ni). This materials degradation is a problem especially for 'cracking tubes' in the ethylene production by pyrolysis of hydrocarbons at 900-1150 °C and $a_C < 1$ but also for heating tubes and other metal components in industrial furnaces for case hardening of steels.

The corrosion phenomenon 'metal dusting' also occurs in these industrial furnaces, but mainly in the chemical and petrochemical industry. Especially the H_2-CO-H_2O-CO_2 atmospheres, produced by methane conversion for synthesis of methanol, ammonia etc. and for the direct reduction of iron ores, caused many failure cases. Metal dusting follows after carbon transfer into metals and alloys, and oversaturation at $a_C > 1$ and is due to the tendency for graphite formation. The mechanisms and kinetics have been studied in depth in the recent years [5-10] and will be presented shortly in this paper.

2 GAS CARBURIZATION

2.1 Kinetics of the Carburizing Reactions

Carbon is transferred into iron by the following reactions:

$$CO + H_2 = H_2O + C \text{ (dissolved)} \qquad (1)$$

$$2\,CO = CO_2 + C \text{ (dissolved)} \qquad (2)$$

$$CH_4 = 2\,H_2 + C \text{ (dissolved)} \qquad (3)$$

The thermodynamics of these reactions is well known [1], their kinetics was investigated in depth since 1965 [11-15], using the resistance-relaxation method or gravimetric measurements of the carburization and decarburization on thin iron foils in flowing gas mixtures (**Figure 1**). On the thin foils the surface reactions were rate controlling and the diffusion equilibrium was virtually established. Here only the main kinetic equations and dependencies will be presented and explained shortly. Reaction (1) is the fastest and most important carburization reaction, and takes place by the reaction steps:

$$CO = CO(ad) = O(ad) + C(dissolved) \qquad (1a)$$

$$O(ad) + H_2 = H_2O \qquad (1b)$$
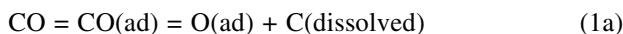
where (ad) means adsorbed. Step (1a) is rate controlling and (1b) is virtually in equilibrium, since its forward and backward reactions are very fast, more rapid than those of step (1a). This follows from the rate equation which was determined experimentally [13-15]:

$$v_1 = k_1 \cdot pCO \cdot \frac{1}{1 + K_O \cdot pH_2O / pH_2} - $$
$$- k'_1 \cdot a_C \cdot \frac{K_O \cdot pH_2O / pH_2}{1 + K_O \cdot pH_2O / pH_2} \qquad (4)$$

where v_1 [mol/cm^2 sec] is the rate of C-transfer, k_1 and k_1' are rate constants, p_i the partial pressures and K_O the equilibrium constant of the adsorption equilibrium $H_2O = H_2 + O(ad)$. The forward reaction rate is proportional to pCO and the part of surface $(1 - \theta_O)$ which is free of O(ad). The backward reaction is proportional to a_C and θ_O, i.e. the degree of coverage with O(ad) which is described by a Langmuir-isotherm:

$$\theta_O = \frac{K_O \cdot pH_2O / pH_2}{1 + K_O \cdot pH_2O / pH_2} \qquad (5)$$

Equation (4) can be written:

$$v_1 = k_1 \cdot pCO \cdot \frac{1}{1 + K_O \cdot pH_2O / pH_2}(1 - a_C / a_C^{eq}) \qquad (6)$$

where a_C^{eq} is the carbon activity in equilibrium with the given gas atmosphere. In the case $K_O \cdot pH_2O/pH_2 \gg 1$ a dependence results on the partial pressures, which is well known from practice:
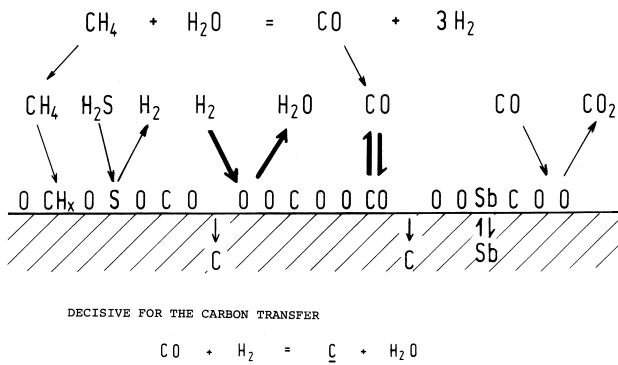
$$v_1 \approx \frac{pCO \cdot pH_2}{pH_2O} \qquad (7)$$

The reaction (2) takes place in the two steps:

$$CO = CO(ad) = O(ad) + C(dissolved) \qquad (2a = 1a)$$

$$O(ad) + CO = CO_2 \qquad (2b)$$
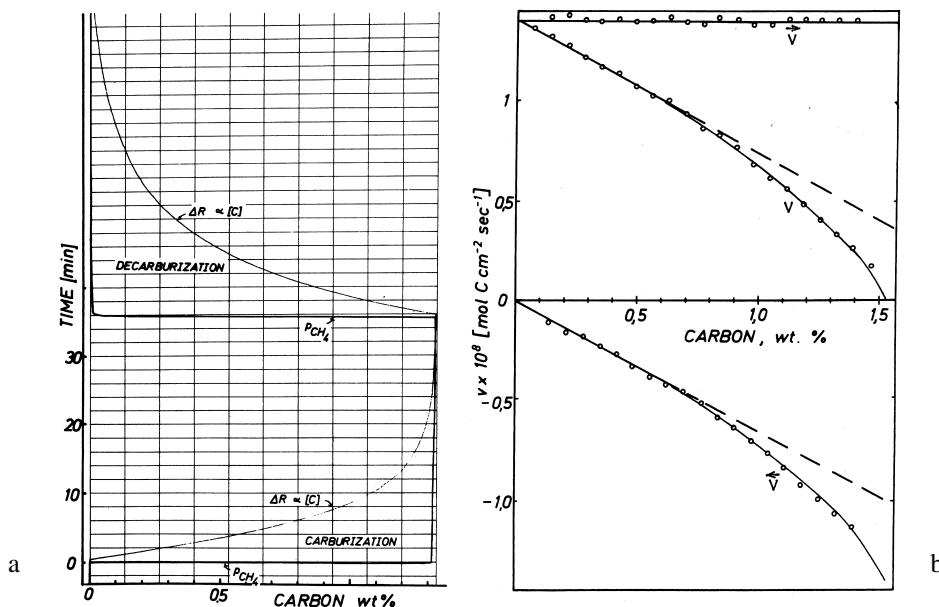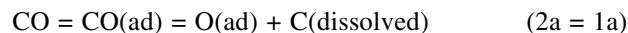
Figure 1: Carburization in CH_4-H_2 and decarburization in H_2 of an iron foil (10 μm) at 1000 °C, resistance-relaxation method [11,12]: a) recorder plot showing change of CH_4 partial pressure and electrical resistance of the foil $\Delta R \sim [C]$ with time, b) evaluation of (a), plot of carburization rate v_3 decarburization $\bar{v}_3$, and forward reaction rate $\vec{v} = v_3 + \bar{v}$

Slika 1: Naogljičenje železne folije (10 μm) v CH_4-H_2 in razogljičenje v H_2 pri 1000 °C, metoda upornosti - relaksacije [11,12]: a) časovni zapis spremembe parcialnega tlaka CH_4 in električna upornost folije $\Delta R \sim [C]$, b) ocena (a), odvisnost od hitrosti naogljičenja v_3, razogljičenje $\bar{v}_3$ in napredovanje hitrosti reakcije $\vec{v} = v_3 + \bar{v}$

$$CH_4 \;+\; H_2O \;=\; CO \;+\; 3\,H_2$$

DECISIVE FOR THE CARBON TRANSFER

$$CO \;+\; H_2 \;=\; \underline{C} \;+\; H_2O$$

Figure 2: Schematics of the partial reactions in gas carburization of iron in a CO-CO$_2$-H$_2$-H$_2$O-CH$_4$-H$_2$S atmosphere, the thickness of the arrows characterizes the reaction velocities, adsorbed or segregated atoms occupy and block reactions sites on the surface
Slika 2: Shema hitrosti parcialnih reakcij. Adsorbirani ali segregirani atomi zasedejo in blokirajo reakcijska mesta pri plinskem naogljičenju železa v atmosferi CO-CO$_2$-H$_2$-H$_2$O-CH$_4$-H$_2$S, debelina puščic je merilo na površini.

Thus the first step, the CO-adsorption and dissociation is the same for reactions (1) and (2). The second step, the removal of O(ad) by reaction with CO, however, is much slower than its removal by reaction with H$_2$, so that the overall reaction (2) is slower than reaction (1). Addition of H$_2$ clearly accelerates the carbon transfer from CO to iron [13-15].

The carbon transfer from CH$_4$, reaction (3) is even very much slower than both reactions (1) and (2), it takes place by stepwise dehydrogenation of the relatively stable molecule CH$_4$ [11,12]. So the carbon transfer from CH$_4$ plays only a negligible role in the carburization of iron in a CO-H$_2$O-CO$_2$-CH$_4$ mixture. The rate equation of reaction (3) determined in the early studies [11,12]

$$v_3 = k_3 \cdot pCH_4/(pH_2)^{1/2} - k'_3 \cdot a_C \cdot (pH_2)^{3/2} \tag{8}$$

indicates that after adsorption of CH$_4$ one H-atom is lost, and the decomposition of adsorbed CH$_3$ becomes rate determining for carburization, for the back reaction CH$_3$ formation is rate controlling. That in fact, the backward reaction rate is proportional to a_C and not to the solute carbon concentration is demonstrated in **Figure 1**, the back reaction rate increases stronger than proportional to the solute concentration, because of the well-known deviation from ideality in the system γ-Fe-C at high carbon concentrations.

The rate constants for the forward reactions were determined on iron at 920 °C [13]:

$k_1 = 7.6 \cdot 10^{-4}$ mol/cm^{2}s bar
$k_2 = 1.5 \cdot 10^{-4}$ mol/cm^{2}s bar
$k_3 = 1.9 \cdot 10^{-6}$ mol/cm^{2}s bar

With this knowledge on the kinetics the atomistic model for carbon transfer results, which is shown in **Figure 2**. Methan conversion by H$_2$O or CO$_2$ needs decomposition of the CH$_4$-molecule [16], either on hot furnace walls as in the case of gas carburization, or by catalytic action e.g. of nickel catalysts. It may be noted that

CH$_4$-decomposition is extremely slow only on iron. Studies on Fe-Ni, Fe-Cr and Fe-Mn foils have shown [17] that the alloying elements cause a drastic increase of the carburization rate. From pure iron to pure nickel k_3 is increasing by two orders of magnitude, therefore Ni is a good catalyst for methane conversion at high temperatures and methane formation at low temperatures.

Case hardening of steels is also conducted by carburization, introducing organic compounds such as methanol, aceton, propanol, acetaldehyde and ethyl acetate [18,19]. These compounds are decomposed at the carburization temperature after short residence time by homogeneous gas reactions, delivering the simple gases CO, H$_2$, CO$_2$, CH$_4$ and H$_2$O so that the carburization will take place, as described mainly by reaction (1). For example methanol decomposes at high temperatures rapidly according to CH$_3$OH $\rightarrow$ CO + 2H$_2$, and carburization experiments showed equal rates, for a certain CH$_3$OH partial pressure in the experiment, and for CO and H$_2$ pressures as resulting from the decomposition of that CH$_3$OH content [18,19].

2.2 Retardation of carburization by adsorbed or segregated elements

The reactions (1) and (3) also have been studied in the presence of some H$_2$S in the flowing gas mixtures. Sulfur is adsorbed on iron very strongly according to

$$H_2S = H_2 + S(ad) \tag{9}$$

Already at relatively low sulfur activities $a_s \sim$ pH$_2$S/pH$_2$ the coverage with S(ad) approaches a monolayer, e.g. at 850 °C at pH$_2$S/pH$_2$ $\approx$ 10^{-6} [20,21]. The adsorbed sulfur atoms are blocking the reaction sites for carbon transfer, similarly as the adsorbed oxygen. Thus with increasing pH$_2$S/pH$_2$ a decrease of carburization rate is observed, for the forward reaction (1) was found:

$$\vec{v}_1 = k_1 \cdot pCO \cdot \frac{1}{1 + K_S \cdot pH_2S/pH_2 + K_O \cdot pH_2O/pH_2} \tag{10}$$

The carbon transfer is only possible on sites which are free of S(ad) and O(ad), see **Figure 2**.

The dependence of $\vec{v}_1$ on sulfur activity was measured in flowing CO-H$_2$-H$_2$S mixtures at 1000 °C, see **Figure 3**. Already at pH$_2$S/pH$_2$ = 10^{-5} the rate is clearly diminished. At higher sulfur activities $\vec{v}_1$ becomes inversely proportional to the sulfur activity, which means the sulfur coverage approaches a monolayer. However the adsorption equilibrium (9) leaves always some vacancies for carbon transfer, up to the sulfur activity, where FeS can be formed (pH$_2$S/pH$_2$ = 5.5·10^{-3} at 1000 °C).

Not only by adsorption but also by segregation from the metal phase a blocking of reaction sites for carbon transfer is possible. This was shown especially for case hardening steels containing antimony [22,23], already relatively small concentrations of about 100 ppm Sb cause a drastic decrease of the carbon transfer
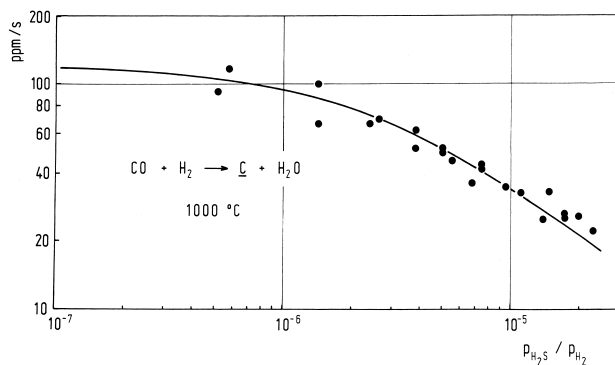
Figure 3: Initial rates of carburization of an iron foil, from resistance-relaxation measurements, conducted in flowing H_2-CO-H_2S mixtures at 1000 °C, as a function of the ratio H_2S/H_2 (sulfur activity)
Slika 3: Začetna hitrost naogljičenja železne folije iz meritev upornosti - relaksacije v toku zmesi H_2-CO-H_2S pri 1000 °C kot funkcija razmerja H_2S/H_2 (aktivnost žvepla)

coefficient. The surface segregation of Sb was demonstrated by surface analytical studies (AES) on Sb-containing steels after heat treatment at 930 °C. Cu, Sn and As are much less effective.

3 HIGH TEMPERATURE CORROSION BY CARBURIZATION

3.1 Internal carbide formation

Carburization of high alloy steels, leading to internal carbide formation, see **Figure 4a**, is a problem in the 'cracking' of hydrocarbons for ethylene production [3,24-27]. At 900 - 1100 °C hydrocarbons and water vapor are passed through the cracking tubes, typical materials for such tubes are steels based on Fe-20Cr-32Ni (Alloy 800) and the cast steels Fe-25Cr-20Ni (HK40) and Fe-25Cr-35Ni (HP40). In the pyrolysis process, carbon is deposited on the tube walls and this 'coke' must be removed repeatedly by decoking with water vapor and air. The tube materials should form protective Cr_2O_3-scales which hinder the ingress of carbon into the steels. Carbon is virtually insoluble in chromia and can be transferred into the steel only by diffusion of molecules through pores and cracks of the scale [28,29]. So cracking tubes can be operated for 5-10 years if critical conditions are avoided. Overheating is critical since Cr_2O_3 is converted to carbide at >1050 °C and at $a_C = 1$ [24-27], as given when the inner wall is covered with coke and heated too high, e.g. upon decoking. There are also tendencies to operate the cracking units at temperatures >1050 °C and it must be emphasized that chromia forming steels are not capable for such operation, - not only the conversion of Cr_2O_3 to carbides at the process gas side but also evaporation of CrO_3 and $CrO_2(OH)_2$ at the fireside will rapidly destroy the tubes [30]. Present alloy development for process operation at >1100 °C aims at Ni-base alloys forming alumina or silica-scales.
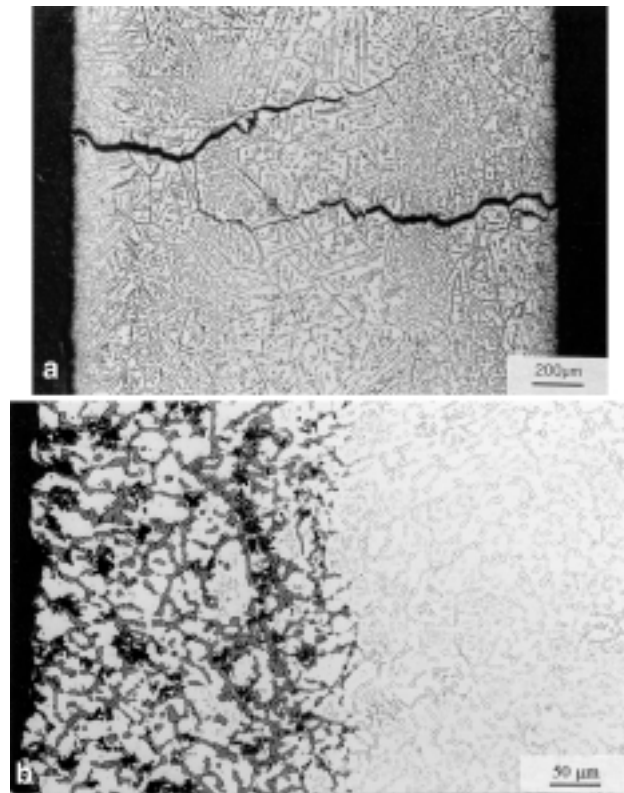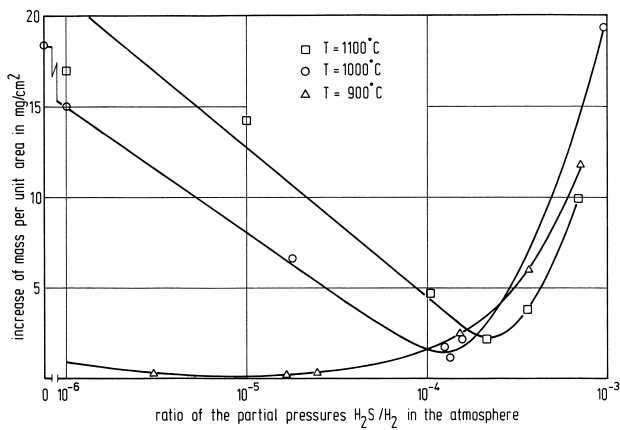

Figure 4: Internal carbide formation in high alloy materials by carburization at $a_C < 1$, metallographic cross sections: a) of a thoroughly carburized Fe-32Ni-20Cr sample (Alloy 800), after carburization in CH_4-H_2 at 1000 °C, crack formation by internal stresses [25,26], b) of the protection tube of an oxygen probe, made of Ni-16Cr-8Fe (Alloy 600), after service in a carburization furnace, internal carbide formation followed by internal oxidation [32].
Slika 4: Nastanek notranjih karbidov v visoko legiranem materialu pri naogljičenju z $a_c < 1$, metalografski prerez: a) popolnoma naogljičen vzorec Fe-32Ni-20Cr (zlitina 800), po naogljičenju v CH_4-H_2 pri 1000 °C. Nastanek razpok zaradi notranjih napetosti [25,26], b) varovalna cev kisikove sonde iz Ni-16Cr-8Fe (zlitina 600) po uporabi v naogljičevalni peči; notranji nastanek karbidov in notranje oksidacije za njim [32].

In normal operation the oxide scale will have defects, by cracking and spalling due to creep of the tubes and due to the thermal cycling, connected with the decoking procedure. To avoid ingress of carbon at these defects, addition of sulfur to the process gases is favourable. Organic sulfur compounds, e.g. dimethyl-disulfide decompose under formation of H_2S, and on free metallic spots the adsorption equilibrium is established. Studies on the carburization of Alloy 800 in CH_4-H_2-H_2S [31] have established the optimum ratios H_2S/H_2 for protection, for 1000 °C the value is $H_2S/H_2 \approx 10^{-4}$, for higher temperatures higher values are necessary, for lower temperatures lower values, see **Figure 5**.

Internal carbide formation also means loss of oxidation resistance since the Cr is tied up in the carbides M_7C_3 and $M_{23}C_6$. Internal oxidation may follow if the material is exposed to oxidizing conditions. The internal carbides are oxidized to Cr_2O_3 and the material

Figure 5: Effect of sulfur on internal carbide formation, mass gain of 20 % Cr - 32 % Ni steel samples after 100 h carburization at 900, 1000 and 1100 °C in CH_4-H_2-H_2S at $a_C = 1$, plotted vs. the varied H_2S/H_2-ratios [31]

Slika 5: Vpliv žvepla na notranji nastanek karbidov, pridobitev na masi vzorcev jekla 20 % Cr - 32 % Ni po 100 urah naogljičenja pri (900, 1000 in 1100) °C v CH_4-H_2-H_2S zmesi in $a_C = 1$ v odvisnosti od različnega H_2S/H_2 razmerja [31]

disintegrates. This phenomenon was called 'green rot', since often nicely green Cr_2O_3 is formed.

Cases of internal carbide formation and green rot have occurred also in furnaces for heat treatment, i.e. in components made of high alloy steels: heating tubes, furnace walls, ventilation wings, protection tubes for thermoelements and oxygen probes, see **Figure 4b**.

3.2 Metal Dusting

Metal dusting is a disintegration of metals and alloys to a dust of metal particles and dust, occurring in strongly carburizing atmospheres at $a_C>1$. The final reason for metal dusting is the tendency for graphite formation $\Delta G = -RT \ln a_C$. Graphite grows after oversaturation of the metal phase with dissolved carbon and destroys the material. The mechanism may involve different steps depending on the material, as described below.

Metal dusting is observed in the colder parts of industrial furnaces for the case hardening of steels. At the carburization temperatures > 900 °C the carbon activity of the CO-H_2-H_2O-CO_2 mixture is $a_C < 1$ but for reactions (1) and (2) a_C increases with decreasing temperature and in colder parts, near the furnace wall or in holes of the wall for thermoelements or oxygen probes the critical condition $a_C>1$ is given, accordingly metal dusting attack was observed, see **Figure 6**. Problems caused by 'syngas' or reduction gas from the conversion of natural gas are widespread, metal dusting attack has been observed in plants for methanol, ammonia, and hydrocarbon production, and in plants for direct reduction of iron ores. But also in hydrocarbons metal dusting is possible and recently problems in refineries have been reported [33].
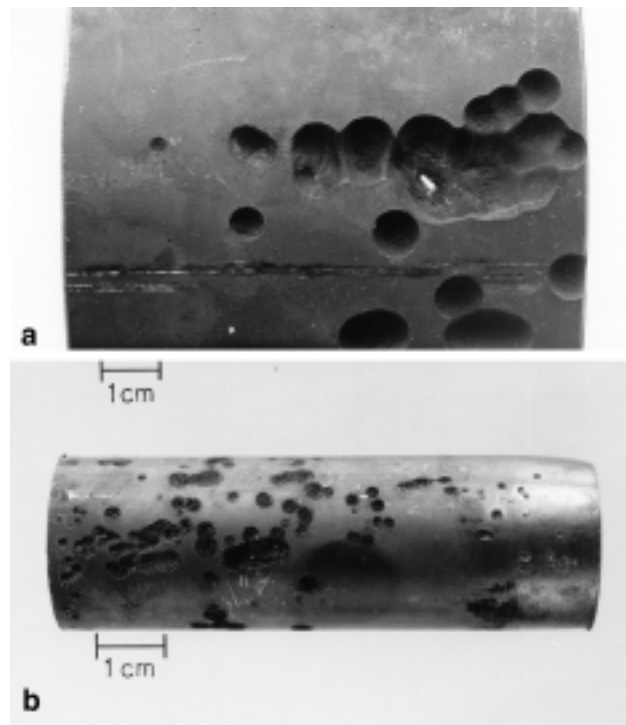
Figure 6 Failure cases by metal dusting in an industrial furnace for gas carburization of case hardening steels, attack of heating tubes in less hot regions of the furnace, where $a_C > 1$: a) austenitic 15Cr-35Ni-steel, b) Ni-16Cr-8Fe (Alloy 600) [7]

Slika 6: Poškodbe zaradi uprašenja kovine v industrijski peči za plinsko naogljičenje jekel za cementacijo, uprašenje ogrevnih cevi v manj vročih delih peči, kjer je $a_C < 1$ a) avstenitno jeklo 15Cr-35Ni, b) Ni-16Cr-8Fe (zlitina 600) [7]

On iron and low alloy steels the attack may start with wide pits but becomes more or less general, so that uniform wastage is observed. The mechanism, see **Figure 7**, involves intermediate formation of the unstable cementite [5-9], the following steps are taking place:

(i) carbon transfer and oversaturation of the metal matrix,

(ii) formation of cementite M_3C (M=Fe,Ni) at the surface and at grain boundaries. The cementite layer is a diffusion barrier for further carbon ingress, causing increase of a_C, and

(iii) nucleation of graphite on the surface, causing decrease of $a_C \rightarrow 1$. The cementite becomes unstable and starts to decompose

(iv) by inward growth of graphite. In the decomposition

$$M_3C \rightarrow 3M + C \qquad (11)$$

the C-atoms attach to graphite planes, which grow more or less vertical into the cementite. The metal atoms migrate through the graphite and agglomerate under formation of fine metal particles (~ 20 mm), which

(v) catalyze carbon deposition from the gas phase, often under growth of carbon filaments from the metal particles.
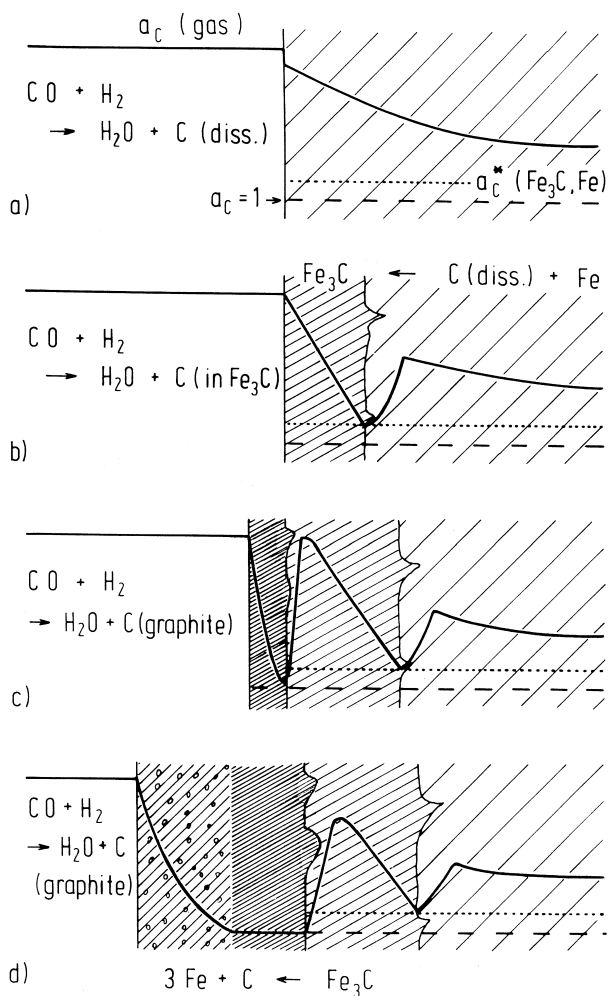
Figure 7: Schematics of the mechanism of metal dusting on iron and low alloy steels [5-9]: a) oversaturation of the metal phase with dissolved carbon, b) growth of cementite at the surface, c) deposition of graphitic carbon on the cementite, $a_C \rightarrow 1$, d) decomposition of the cementite, and carbon deposition by catalytic action of the metal particles, arising from cementite decomposition

Slika 7: Shema mehanizma uprašenja železa in malo legiranih jekel [5-9]: a) prenasičenje kovinske faze z raztopljenim ogljikom, b) rast cementita na površini, c) nanos grafita na cementitu, $a_C \rightarrow 1$, d) razpad cementita in nanos ogljika s katalitsko reakcijo zrn kovine, ki so nastale z razpadom cementita

The steady state of this mechanism is demonstrated in **Figure 8**.

On high alloy steels and Ni-base alloys with sufficient Cr-content generally an oxide layer is formed and metal dusting starts locally, at defects where the layer has a crack or pore or has spalled. In these materials an internal carbide formation takes place at first, the chromium carbides $M_{23}C_6$ and M_7C_3 precipitate and the carbides of other stable carbide formers such as Ti, Nb, W, Mo etc. This process causes some delay of the oversaturation and the start of metal dusting (which is however not significant, considering the requested life times). A fringe with precipitates is formed around the point of attack. In the temperature range about 600 °C
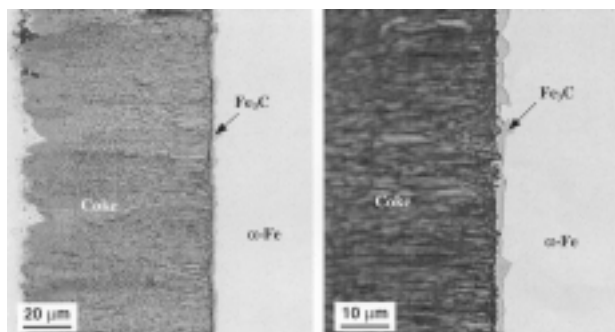

Figure 8: Metallographic cross section of an iron sample after 4 hours metal dusting in 30 % CO - 70 % H_2 - 0,2 % H_2O at 600 °C, optical micrograph demonstrating the steady state of inward cementite growth and Fe_3C decomposition by growth of graphite into the cementite, outward coke formation

Slika 8: Metalografski prerez vzorca železa po 4 urah kovinskega uprašenja v 30 % CO - 70 % H_2 - 0,2 % H_2O pri 600 °C. Optični posnetek dokazuje stabilno rast cementita v notranjost in razpad Fe_3C z rastjo grafita v cementit, navzven nastanek koksa.
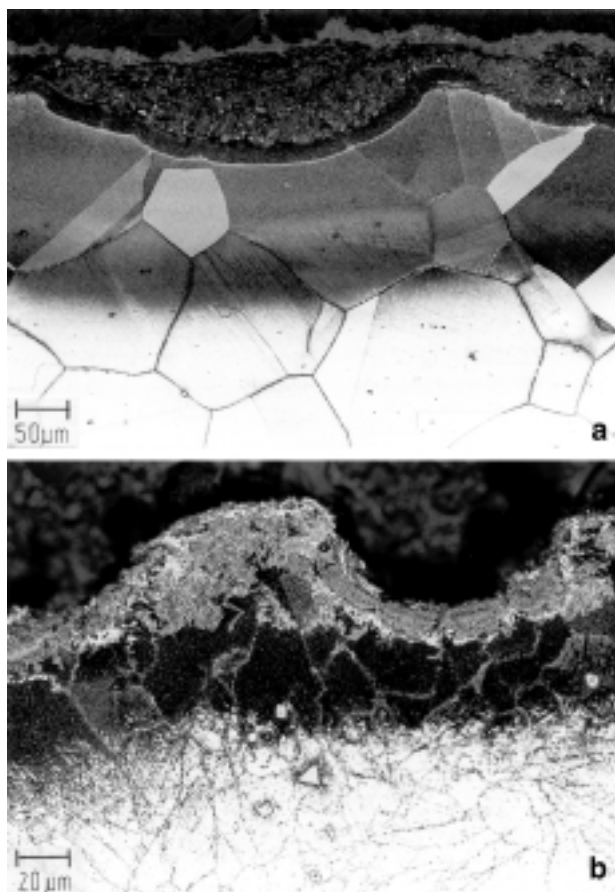
Figure 9: Metallographic cross sections of alloys attacked by metal dusting: a) Fe-20Cr-32Ni (Alloy 800) with carburized zone and "coke" in the pits, b) Ni-16Cr-8Fe (Alloy 600), same protection tube as in **Figure 2b**, but in a region of lower temperature $a_C > 1$

Slika 9: Metalografski obrus zlitin napadenih s prašenjem kovine: a) Fe-20Cr-32Ni (zlitina 800) z naogljičeno zono in koksom v zajedah, b) Ni-16Cr-8Fe (zlitina 600), ista varovalna cev kot na **sliki 2b**, vendar področje z nižjo temperaturo $a_C > 1$
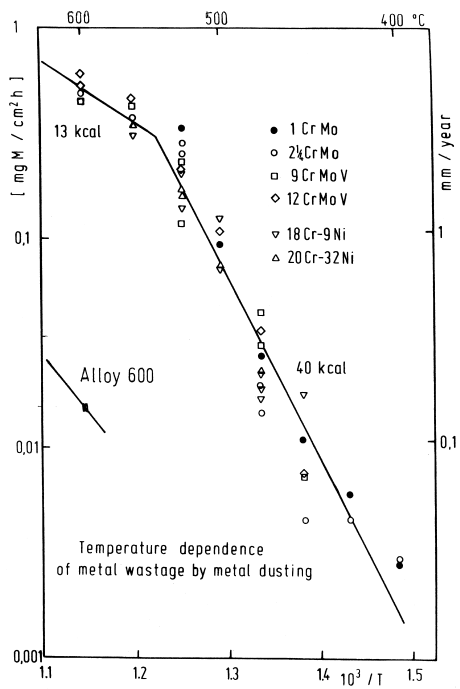
Figure 10: Arrhenius-plot of wastage rates by metal dusting of several steels and Ni-base alloy 600 versus reciprocal temperature (K^{-1}), the data were determined in H$_2$ - 24 % CO - 2 % H$_2$O when the attack on the surface was uniform [9]

Slika 10: Arrheniusov diagram odvisnosti hitrosti prašenja več jekel in nikljeve zlitine 600 od recipročne temperature (K^{-1}), podatki iz H$_2$ - 24 % CO - 2 % H$_2$O v primeru enakomernega prašenja površine [9]

which is most critical concerning appearance of metal dusting, these precipitates are very fine and the etched metallographic cross section shows only a dark zone, see **Figure 9**. The local attack spreads and leads to formation of pits, which are more or less hemispherical. In laboratory experiments worms of coke can be seen, growing from each pit. In industrial units the coke is mostly carried away by the fast flowing process gases, and can be found deposited in bends or dead ends of the system.

It should be noted that the metal dusting mechanism for Ni and Ni-base alloys is different from that for iron and steels. No unstable carbide is formed as intermediate but the graphite directly grows into the oversaturated metal and destroys the materials [34,35].

The difference in the mechanism for steels and Ni-base Alloy 600 can be seen also in the Arrhenius-diagram **Figure 10**, which collects rates of metal consumption measured on samples which were corroding on their whole surface. The Arrhenius-line for the steels yields an activation energy of about 167 kJ/mol for the temperature range up to about 540 °C, and that value most probably can be attributed to reaction (11), i.e. the cementite decomposition. At higher temperatures a lower activation energy was found, about 55 kJ/mol which probably is valid for the carbon transfer reaction, here reaction (1). This assumption would be

well in agreement with the partial pressure dependence of the metal consumption, which is v ~ pCO·pH$_2$ [10], corresponding to the well-known dependence of the carbon transfer coefficient as already given in equation (7).

The carbon deposition, according to step (v) of the above reaction mechanism was found to be proportional to pCO and to increase quadratically with time [6], which follows if it is assumed that the deposition is proportional to the amount of metal particles formed in step (iv). Carbon deposition is generally higher for the austenitic materials compared to the ferritic steels, and its activation energy contains the activation energy for the formation of the catalytic particles reaction (11). The complex processes in the metal dusting of iron and steels, however, are not fully understood. Changes of the mechanism result from a change of morphology of the reaction products with temperature. At > 700 °C the cementite decomposition reaction (11) can result in formation of a dense iron layer on the cementite, see **Figure 11**, through which the carbon must diffuse for graphite growth [36,37]. Then carbon diffusion in the iron layer becomes rate controlling and the velocity and severity of metal dusting is drastically decreased.

3.3 Effects of Sulfur on Corrosion by Carbon

While the retarding effect of sulfur is unwanted in the gas carburization of steels, this effect is welcome on carburization as a high temperature corrosion process. Additions of sulfur bearing compounds is used in the ethylene production by cracking of hydrocarbons. A quantitative study using CH$_4$-H$_2$-H$_2$S mixtures for carburization of Alloy 800 in the temperature range 900 - 1100 °C, see **Figure 5**, showed that at 1000 °C the carburization and internal carbide formation is
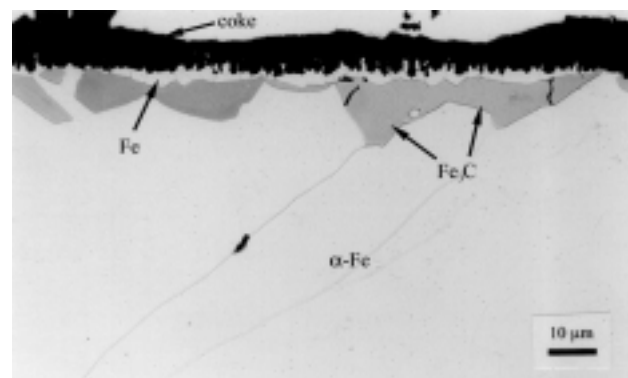
Figure 11: Metallographic cross section of an iron sample after 4 hours in H$_2$ - 5 % CO - 0,2 % H$_2$O at 700 °C, optical micrograph showing inward growth of cementite and its outward decomposition under iron layer formation, the carbon diffuses through this layer so that graphite grows into the iron layer

Slika 11: Metalografski obrus vzorca železa po 4 urah v H$_2$ - 5 % CO - 0,2 % H$_2$O pri 700 °C. Optični posnetek prikazuje rast cementita v notranjost in njegov razpad proti zunanjosti pod nastajajočim slojem železa. Ogljik difundira skozi ta sloj, zato grafit raste v sloj železa.
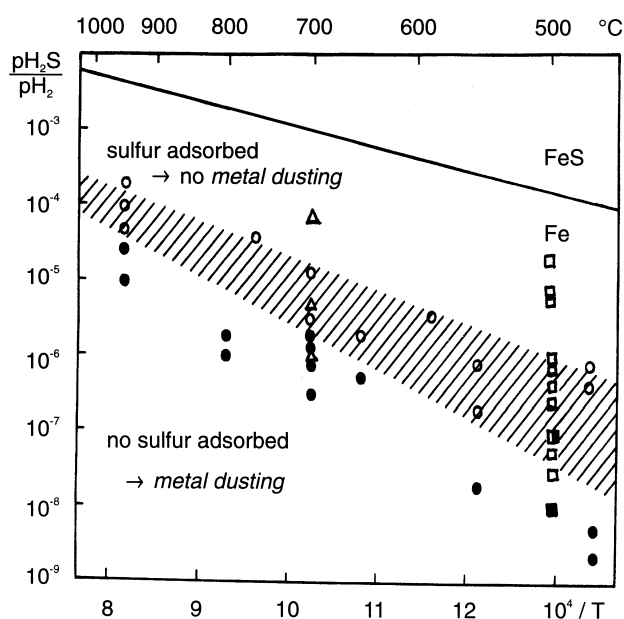
Figure 12: Thermodynamic plot on the effect of sulfur on the occurrence of metal dusting, $log(pH_2S/pH_2)$ versus $1/T$, presenting the regions with low sulfur coverage and fast occurrence of metal dusting (black dots), and regions where monolayer coverage with S(ad) is approached (hatched), and region with monolayer coverage - in both the latter regions metal dusting is effectively suppressed, uppermost field - FeS stable [40,41].

Slika 12: Termodinamična odvisnost vpliva žvepla na pojav uprašenja kovine, $log(pH_2S/pH_2)$ v odvisnosti od $1/T$, ki prikazuje področje z majhnim žveplovim prekritjem, hiter pojav uprašenja kovine (črne točke) in področja, kjer je doseženo približno enoatomsko pokritje z S(ad) (šrafirano) in področja z doseženim enoatomskim prekritjem. Na obeh področjih je učinkovito preprečeno uprašenje, zgornje polje - stabilen FeS [40,41].

suppressed optimally at $pH_2S/pH_2 \cong 10^{-4}$, at higher ratios the material is endangered by sulfidation of the alloying elements Cr and Mn. From the kinetic studies of reactions (1) and (3), it was known already [20,21] that for this ratio the rate of carbon transfer is decreased by two orders of magnitude, compared to the rate in absence of sulfur. As known from studies about adsorption and segregation of sulfur on iron [38,39] for such H_2S/H_2 ratio at 1000 °C the coverage with S(ad) approaches a monolayer, see **Figure 12**.

Presence of sulfur is also an effective remedy against metal dusting. Adsorbed sulfur hems the carbon transfer, step (i) of the metal dusting mechanism, but in addition it suppresses step (iii), the nucleation of graphite effectively. To nucleate graphite, an ensemble of free sites is necessary and even if the coverage with sulfur is much less than a monolayer, graphite nucleation cannot take place. Thus, the carbon activity on the cementite layer stays high and its decomposition cannot start. Continued cementite growth has been observed in $CO-H_2-H_2O-H_2S$ or $CH_4-H_2-H_2S$ mixtures. Generally the stability of cementite achieved depends on the carbon activity and time of exposure, but a diagram was derived from studies on iron and low alloy steels, describing, the ranges of

immediate metal dusting and suppressed metal dusting, i.e. continued cementite growth, in dependence on pH_2/pH_2 and $1/T$, see **Figure 12** [40,41]. In the range of low pH_2S/pH_2 the coverage with S(ad) is very low and not sufficient to suppress metal dusting for long time. In the hatched range of conditions the monolayer coverage is approached ($\theta = 0.90-0.99$) and the start of metal dusting is effectively retarded. In the range of high pH_2S/pH_2 no metal dusting occurs and cementite is largely stabilized. It may be noted that the hatched area at high temperatures 900-1100 °C corresponds to the pH_2S/pH_2-values determined to be optimal for retardation in the carburization of high temperature alloys.

Furthermore the 'stabilization of cementite' is of great scientific interest to study properties of the otherwise unstable compound and for example to determine diffusivities of C in Fe_3C from its growth rate. And the growing of cementite also has important practical interest, since cementite would be a valuable product in the direct reduction of iron ores. This 'iron carbide production' has been studied in detail [42-45] and also tried in large scale but with no great success. Iron carbide would be a valuable raw material for the use in steel production in electric furnaces.

4 REFERENCES

[1] Grabke, H.J.; Grassl, D.; Hoffmann, F.; Liedtke, D.; Neumann, F.; Schachinger, H.; Weissohn, K.H.; Wünning, A.: Wyss, U.; Zoch, H.-W. (AWT-Fachausschuss 5, Arbeitskreis 4): Die Prozessregelung beim Gasaufkohlen und Einsatzhärten. Renningen-Malmsheim: expert-Verlag, 1997

[2] Grabke, H.J.: Härterei-Techn. Mitteilungen 45 (**1990**) 2, 110-118

[3] Grabke, H.J.: MIT Publication No. 52, Materials Technology Institute of the Chemical Process Industries Inc. St. Louis, 1998

[4] Grabke, H.J.: Mat. at High Temperatures 17, 4 (**2000**) 1

[5] Grabke, H.J.; Krajak, R.; Müller-Lorenz, E.M.: Werkst. u. Korr. 44 (**1993**) 89-97

[6] Grabke, H.J.; Bracho-Troconis, C.B.; Müller-Lorenz, E.M.: Werkst. u. Korr. 45 (**1994**) 215-221

[7] Grabke, H.J.; Krajak, R.: Härterei-Techn. Mitteilungen 49 (**1994**) 2

[8] Grabke, H.J.:, Mat. Corr. 49 (**1998**) 303-308

[9] Grabke, H.J.; Müller-Lorenz, E.M.: Mat. Corr. 49 (**1998**) 317-320

[10] Müller-Lorenz, E.M.; Grabke, H.J.: Mat. Corr. 50 (**1999**) 614-621

[11] Grabke, H.J.: Ber. Bunsenges. Physik. Chemie 69 (**1965**) 409-14

[12] Grabke, H.J.: Metallurg. Trans. 1 (**1974**) 2972-2975

[13] Grabke, H.J.: Archiv Eisenhüttenwesen 46 (**1975**) 75-81

[14] Grabke, H.J.; Tauber, G.: Archiv. Eisenhüttenwes. 46 (**1975**) 215

[15] Shatynski, S.R.; Grabke, H.J.: Archiv Eisenhüttenwes. 49 (**1978**)129

[16] Münster, P.; Grabke, H.J.: Ber. Bunsenges. physik. Chemie 4 (**1980**) 1068

[17] Grabke, H.J.; Müller, E.M.; Speck, H.V.; Konczos, G.: Steel Research 56 (**1985**) 275

[18] Speck, H.V.; Grabke, H.J.; Müller, E.M.: Härterei-Techn. Mitteilungen 40(**1985**) 92-103

[19] Speck, H.V.; Grabke, H.J.: Chem.-Ing.-Tech. 56 (**1984**) 642

[20] Grabke, H.J.; Petersen, E.M:; Srinivasan, S.R.: Surf. Sci. 67 (**1977**) 501

[21] Grabke, H.J.: Mater.Sci. Eng. 42 (**1980**) 91

[22] Ruck, A.; Monceau, D.; Grabke, H.J.: Steel Research 67 (**1996**) 240

[23] Grabke, H.J.: Kovine, zlitine, tehnologije 30 (**1996**) 483-495

[24] Grabke, H.J.; Gravenhorst, U.; Steinkusch, W.: Werkst. u. Korr. 27 (**1976**) 291

[25] Schnaas, A.; Grabke, H.J.: Oxidation of Metals 12 (**1978**) 387

[26] Grabke, H.J.; Schnaas, A.: In Alloy 800, Betteridge W. et al. (eds). North-Holland: Amsterdam, (**1978**) 195-211

[27] Schnaas, A.; Grabke, H.J.: Werkst. Korros. 29 (**1978**) 635

[28] Grabke, H.J.; Wolf, I.: Mat. Sci. Eng. 87 (**1987**) 23

[29] Wolf, I.; Grabke, H.J.; Schmidt, P.: Oxidation of Metals 29 (**1988**) 289.306

[30] Grabke, H.J.; Jacobi, D.: Materials and Corrosion 53 (**2002**) 494

[31] Grabke, H.J.; Möller, R.; Schnaas, A.: Werkst. Korros. 30 (**1979**) 794

[32] Grabke, H.J.: Materials and Corrosion 52 (**2001**) 546-551

[33] Grabke, H.J.; Gerk, C.: EUROCORR '99 Aachen CD-Rom. Dechema: 1999

[34] Schneider, R.; Pippel, E.; Woltersdorf, J.; Strauß, S.; Grabke, H.J.: Steel Research 68 (**1997**) 326-332

[35] Grabke, H.J.: Corrosion 56, No. 8 (**2000**) 801-808

[36] Forseth, S., unpublished

[37] Schneider, A.: Corrosion Science 44 (**2002**) 2353-2365

[38] Oudar, J.: Mater. Sci. Eng. 42 (**1980**) 101

[39] Grabke, H.J.; Paulitschke, W.; Tauber, G.; Viefhaus, H.: Surf. Sci. 63 (**1988**) 377

[40] Grabke, H.J.; Müller-Lorenz, E.M.: Steel Research 66 (**1995**) 254-258

[41] Schneider, A.; Viefhaus, H.; Inden, G.; Grabke, H.J.; Müller-Lorenz, E.M.: Mat. Corr. 49 (**1998**) 330-335

[42] Hayashi, S.; Iguchi, Y.: ISIJ Int. 37:16 (**1997**) 345

[43] Iguchi, Y.; Sawai, S.; Ohiwa, K.: Belton Memorial Proc., Sydney, Australia, Jan. 2000, 75

[44] Zhang, J.; Ostrowski, O.: Ironmaking Conf. Proc. 2000, 339

[45] Zhang, J.; Ostrowski, O:: ISIJ Int. 41 (**2001**) 340-344